Available online at www.sciencedirect.com
SCIENCE DIRECT®
PERGAMON
International Journal of Heat and Mass Transfer 46 (2003) 2077–2085
International Journal of HEAT and MASS TRANSFER
www.elsevier.com/locate/ijhmt

On the impingement heat transfer of an oblique free surface plane jet

Albert Y. Tong *

Department of Mechanical and Aerospace Engineering, University of Texas at Arlington, P.O. Box 19023, Arlington, TX 76019, USA

Received 6 May 2002; received in revised form 11 October 2002

Abstract

The objective of the present study is to understand the hydrodynamics and heat transfer of the impingement process, particularly the complexities attributable to the asymmetric geometry of an oblique liquid plane jet. The Navier–Stokes equations are solved using a finite-volume formulation with a two-step projection method on a fixed non-uniform rectangular grid. The free surface of the jet is tracked by the volume-of-fluid method with a second order accurate piecewise-linear scheme. The energy equation is modeled by using an enthalpy-based formulation. The method provides a state-of-the-art comprehensive model of the dynamic and thermal aspects of the impinging process. Nusselt number plots and pressure distributions on the substrate are obtained. The locations of the maximum Nusselt number as well as maximum pressure on the surface are identified and compared with the geometric jet impingement point. Results for normal impingement are also obtained and are used as reference. The effects of several parameters are examined. These include jet Reynolds number, jet impingement angle and jet inlet velocity profile. Experimental and analytical data from the literature are also included for comparison.

1. Introduction

Impinging jets are an established technique for providing high local heat transfer coefficients between a fluid and a surface. A considerable amount of research on impingement heat transfer, both in analytical and experimental aspects, has been published. The majority of the available information on the heat transfer characteristics of impinging jets is on normal impingement. Studies of heat transfer from a jet impinging at an oblique angle to a surface have received relatively little attention. This is perhaps a reflection on the fact normal impingement has more widespread applications. Nevertheless, oblique jet impingement occurs in many applications and a fundamental understanding of the complexities of the hydrodynamics and the heat transfer of the impingement process attributable to the asymmetric geometry is of importance.

In [1], experiments were performed in which a circular jet of air at room temperature was directed obliquely at a plane impingement surface. The surface was a naphthalene plate, which sublimed in response to the airflow passing over it. Highly localized measurements of the mass transfer rates were performed and local mass transfer coefficients were evaluated. The point of maximum mass transfer was found to shift from the geometrical impingement point of the jet, with the extent of the displacement increasing as the inclination increased. The largest displacement encountered during the experiments was about $2\frac{1}{4}$ jet orifice diameters. The local coefficients on the upstream side of the maximum point drop off more rapidly than do those on the downstream side, and this is accentuated at larger inclinations. The values of the maximum coefficient decrease moderately with increasing inclination angle. The greatest decreases encountered were in the 15–20% range. By means of analogy, the mass transfer results are applicable for heat transfer calculations.

In [2], experiments employing temperature-sensitive liquid crystal were conducted to determine the heat

* Tel.: +1-817-272-2297; fax: +1-817-272-2952.
E-mail address: tong@uta.edu (A.Y. Tong).

0017-9310/03/$ - see front matter © 2003 Elsevier Science Ltd. All rights reserved.
doi:10.1016/S0017-9310(02)00505-7

Nomenclature

C_p	specific heat at constant pressure	Re	Reynolds number (UW/v)
D	displacement (upstream)	S	strain rate tensor
F	VOF function (fluid fraction)	T	temperature
F_b	body force	t	time
g	gravitational acceleration	U	average jet inlet velocity
h	enthalpy	V	velocity
k	thermal conductivity	W	jet width
Nu	Nusselt number	X	horizontal coordinate
Nu_{max}	maximum Nusselt number	Z	vertical coordinate
Nu_{stag}	stagnation-point Nusselt number	μ	dynamic viscosity coefficient
P	pressure	ρ	density
P_{max}	maximum pressure	σ	surface tension coefficient
Pr	Prandtl number	τ	viscous stress tensor
q	heat flux		

transfer to a circular air jet impinging at different oblique angles to a plane surface. Contours of constant heat transfer coefficient were presented and correlated with an empirical equation that permits determination of average Nusselt numbers over areas of interest. As in [1], the results indicate a displacement of the peak heat transfer from the geometric center of the jet with the displacement being a function primarily of the impingement angle. A decrease of up to 30% in peak heat transfer was reported.

A series of experiments for the measurement of local heat transfer coefficients for an obliquely impinging circular air jet were reported in [3]. It was also found that for a given flow situation the point of maximum heat transfer shifts away from the geometrical impingement point toward the compression (upstream) side of the wall jet on the axis of symmetry. The shift is more pronounced with a smaller oblique angle (larger jet inclination) and a smaller jet-to-plate distance.

The air jets discussed above are classified as submerged jets where entrainment is important. On the other hand, liquid jet in air is treated as a free jet where the effect of entrainment is negligible and the jet forms a free surface. Two experimental studies [4,5] on oblique liquid jet impingement heat transfer are found in the literature. In [4], the effect of jet inclination on the heat transfer under a round, single-phase free liquid water jet impinging on a flat, constant heat-flux surface was examined. The shape of the local Nusselt number profiles was increasingly asymmetric with a progressive sharpening of the peak as the inclination increases. It was found that the point of maximum heat transfer shifted upstream as has been observed for air jets. However, the magnitude of the shift was significantly less than that of the air jets at similar jet inclinations. Also, contrary to the air jet results, the magnitude of the peak heat transfer was seen to increase slightly with increasing jet inclination. These differences were attributed to the relative unimportance of entrainment and pre-impingement jet spreading for free liquid jets.

In [5], an experimental study was performed to investigate the local heat transfer from a vertical heated surface to an obliquely impinging circular free-surface liquid jet of large Prandtl number. The magnitude of the shifts was again significantly less than that reported for oblique air jets. It should be noted that, contrary to [4], the maximum local Nusselt number was found to diminish with increasing jet inclination. This apparent contradiction in findings between the two studies [4,5] warrants further investigation.

Examination of the relevant literature reveals no prior theoretical (analytical and numerical) study on the local heat transfer under an obliquely impinging, axisymmetric free liquid jet. The only related theoretical work is the paper by Schach [6], which studied the oblique impingement of a free surface liquid plane jet. It was done analytically using the hodograph technique with the hydrodynamic aspect of impingement being the main focus. Solutions for the free surface and the stagnation point location were reported along with numerical results on stagnation point shift and film thickness at several inclination angles. The study, besides being limited to two-dimensional plane flows for an ideal fluid, also requires the jet inlet velocity to be uniform in order to satisfy the irrotational condition for potential flows.

With advances in computers, numerical solutions play an increasingly important role in scientific research. The numerical simulation of the liquid jet impingement is not at all trivial. The main complexity is the dynamics of a rapidly moving free surface, which has long proven to be a difficult problem. The location of the boundary is unknown and is desired as part of the solution. The

difficulty is that the free surface deforms while the values of the field variables are being solved. From a computational standpoint, this presents some very serious issues depending on the solution method used.

Recently, the problem of normal incidence impact with solidification of a spherical liquid metal droplet onto a rigid substrate was investigated by the author and coworkers [7–10]. The motivation for that study came from liquid metal jetting application in electronic manufacturing, much like the technology of ink jet printing. A comprehensive model of the dynamic and thermal aspect of the impact process was developed. The continuity and the Navier–Stokes equations were solved by using a finite-volume formulation on a fixed grid with a two-step projection method. Free surfaces were tracked by a technique called volume-of-fluid (VOF). The energy equation was modeled by using an enthalpy-based formulation. The numerical results were in close agreement with experimental data. The same algorithm was later extended to study the head-on collision behavior of water droplets [11].

The purpose of this investigation is to study numerically the hydrodynamics and heat transfer of an oblique plane jet impinging onto a substrate by applying the above-mentioned free surface flow model. The goal is to understand the heat transfer mechanism of the impingement process, particular the complexities attributable to the asymmetric geometry of the oblique free liquid jet. An oblique circular jet, which involves true three-dimensional modeling, requires considerable computational and programming resources. An oblique plane jet is studied instead. The physics of the impingement process revealed for the plane jet will provide useful information for the circular jets. The inherent difference due to geometry will be discussed.

The VOF scheme used in the previous studies has been replaced by a more accurate piecewise linear scheme in the present study. A brief overview of the numerical formulation is given next, followed by Results and discussion section. Details on the numerical formulation and the piecewise linear scheme can be found in [10] and [12], respectively.

2. Numerical formulation

For incompressible fluids, the continuity and momentum equations are given by

$$\nabla \cdot \vec{V} = 0 \tag{1}$$

and

$$\frac{\partial \vec{V}}{\partial t} + \nabla \cdot (\vec{V}\vec{V}) = -\frac{1}{\rho}\nabla p + \frac{1}{\rho}\nabla \cdot \tau + \vec{g} + \frac{1}{\rho}\vec{F}_b \tag{2}$$

respectively. For Newtonian fluids, we have

$$\tau = 2\mu S \quad \text{and} \quad S = \tfrac{1}{2}[(\nabla \vec{V}) + (\nabla \vec{V})^T] \tag{3}$$

where S is the rate-of-strain tensor. Combining Eqs. (2) and (3) gives the Navier–Stokes equations. Eq. (2) is approximated with a finite-difference in time as

$$\frac{\vec{V}^{n+1} - \vec{V}^n}{\delta t} = -\nabla \cdot (\vec{V}\vec{V})^n - \frac{1}{\rho^n}\nabla p^{n+1} + \frac{1}{\rho^n}\nabla \cdot \tau^n + \vec{g}^n + \frac{1}{\rho^n}\vec{F}_b^n \tag{4}$$

where the superscripts n and $n+1$ represent the value of the variable at consecutive time steps. It is decomposed into the following two equations:

$$\frac{\vec{\tilde{V}} - \vec{V}^n}{\delta t} = -\nabla \cdot (\vec{V}\vec{V})^n + \frac{1}{\rho^n}\nabla \cdot \tau^n + \vec{g}^n + \frac{1}{\rho^n}\vec{F}_b^n \tag{5}$$

and

$$\frac{\vec{V}^{n+1} - \vec{\tilde{V}}}{\delta t} = -\frac{1}{\rho^n}\nabla p^{n+1} \tag{6}$$

where $\vec{\tilde{V}}$ represents an intermediate value of the velocity. The basic algorithm is the two-step projection method in which a time discretization of the momentum equation, Eq. (4), is broken up into two equations, Eqs. (5) and (6). In the first step, an intermediate velocity field, $\vec{\tilde{V}}$, is computed from Eq. (5) which accounts for incremental changes resulting from viscosity, advection, gravity, and body forces. In the second step, the velocity field, $\vec{V}^{n+1}$, is projected onto a zero-divergence vector field resulting in a single Poisson equation for the pressure field given by

$$\nabla \cdot \left[\frac{1}{\rho^n}\nabla p^{n+1}\right] = \frac{\nabla \cdot \vec{\tilde{V}}}{\delta t} \tag{7}$$

which is solved by using an incomplete Cholesky conjugate gradient technique [13].

Free surfaces are tracked by the VOF method. The VOF technique, pioneered by Hirt and Nichols [14], provides a means of following fluid regions through an Eulerian mesh of stationary cells. The basis of the VOF method is the fractional VOF scheme for tracking free boundaries. The governing equation in this method is given by

$$\frac{\mathrm{D}F}{\mathrm{D}t} = \frac{\partial F(\vec{x},t)}{\partial t} + \vec{V} \cdot \nabla F(\vec{x},t) = 0 \tag{8}$$

where F is defined as the volume fraction of fluid whose value is unity at any point occupied by fluid and zero elsewhere. When averaged over a computational cell, it is equal to the fractional volume of the cell occupied by fluid. In particular, a unit value of F corresponds to a cell full of fluid, whereas a zero value indicates that the cell contains no fluid. A cell with F values between 0 and

1 contains a free surface. In addition to defining which cells contain a boundary, the F function can be used to determine the fluid location within a boundary cell.

In the present study, the Nichols–Hirt VOF method, which utilizes a piecewise-constant interface, has been replaced by a more robust Youngs' VOF scheme [15], which uses a piecewise-linear interface. The original paper by Youngs had little detail of the methods by which the interface was reconstructed and fluxes calculated. The algorithm recently outlined by Rudman [12] for the Youngs' VOF scheme has been implemented into the code.

A non-conventional approach called continuum surface force (CSF) method is used to model surface tension [16]. The CSF method interprets surface tension as a continuous, three-dimensional effect across an interface rather than as a boundary value condition at the interface. Interfaces between fluids of different properties (called colors) are represented as transition regions of finite thickness. Across this region there is a continuous variation of the property value of one fluid to the property value of the other fluid. At each point in the transition region, a force density is defined which is proportional to the curvature of the surface of constant property at the point. It is normalized so that the conventional description of the surface tension on an interface is recovered when the ratio of local transition region thickness to local radius of curvature approaches zero.

Heat transfer is governed by an enthalpy-based energy equation given by

$$\frac{\partial \rho h}{\partial t} + \nabla \cdot (\rho \vec{V} h) = \nabla \cdot (\alpha \nabla h) \tag{9}$$

where $\alpha = k/C_p$. The enthalpy formulation is particularly attractive for multiphase flow problems involving phase change. In that case, a source term accounting for the latent heat will be added. Such a simulation was used by the author in the previous studies [7–10].

3. Results and discussion

A schematic of a liquid jet impinging obliquely onto a hot surface is shown in Fig. 1a. The computational boundary conditions are given in the figure. The geometric center of the impinging jet is represented by the dotted line with point C the geometric center of jet impingement at the surface. In most of the simulations, a computational domain of $X = 24$ mm and $Z = 6$ mm is used. The jet width W is kept at 2 mm. The geometric center of the impinging jet is located at the middle, splitting the horizontal axis evenly. It has been found that further extension of X produces practically no change in the flow field. Note that the flow is predominantly parabolic in nature, particularly away from the stagnation region. The influence from both ends is very minimal.

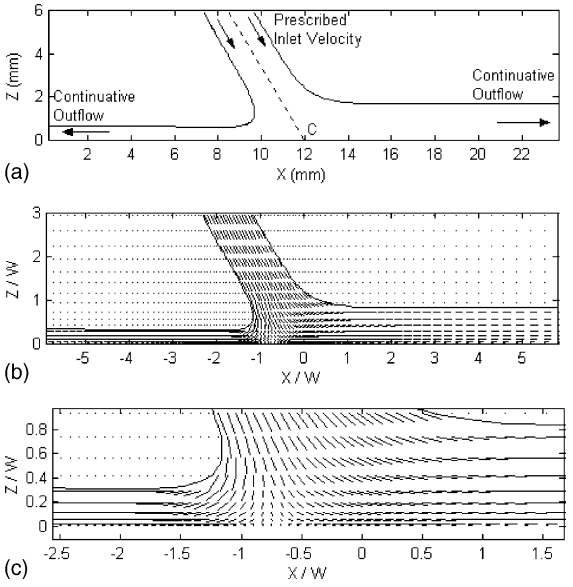

Fig. 1. (a) A schematic of the overall computational domain (top). (b) A sample flow field (middle). (c) Magnified view at the stagnation region (bottom).

A sample flow field for a 60-deg inclination uniform jet is shown in Fig. 1b where the axes have been non-dimensionalized. A magnified view of the flow at the stagnation region is shown in Fig. 1c. Note that the stagnation point is shifted upstream from the geometric center of the jet, in agreement with the results reported in the literature for circular jets previously mentioned.

A non-uniform rectangular grid focusing on the stagnation region is used. In the vertical direction, grid size increases geometrically from bottom to top. In the horizontal direction, fine grids are used at the stagnation-point region and the grid size increases geometrically sideway. A grid refinement study is performed in each case. The grid size is reduced until there is no significant change in the numerical results. Water at standard atmospheric condition with constant thermo-fluid properties is considered. The values used in the numerical simulations are given in Table 1. Since the Prandtl number is much greater than one, the thermal boundary layer is much thinner than the velocity boundary layer and consequently dictates the grid size required for resolution.

Table 1
Thermo-fluid properties of water

Density	1000 kg/m^3
Kinematic viscosity	0.89×10^{-6} m^2/s
Surface tension	7.28×10^{-2} N/m
Specific heat	4.2 kJ/kg K
Thermal conductivity	0.674 W/m K
Prandtl number	5.545

Prior to the presentation of results, with a view to demonstrate the accuracy of the present numerical solutions, comparisons are made with data available in the literature for the case of normal impingement. For a planar uniform jet, exact solution for the inviscid flow in terms of complex velocity potential exists. It was shown [17] that the variation of free stream velocity along the plate could be approximated by

$$\frac{V}{U} = \frac{\pi}{4}\frac{X}{W} \quad \text{for } \frac{X}{W} \leqslant 1.1 \tag{10}$$

As discussed in [17], the following expression for the stagnation point Nusselt number can be derived by using Eq. (10) along with a similarity solution for a Falkner–Skan flow in the stagnation region

$$Nu_{\text{stag}} = 0.505 Re^{0.5} Pr^{0.376} \tag{11}$$

It was mentioned that the correlation was in agreement with laminar jet measurements.

In [18], a theoretical study on the flow and heat transfer of a two-dimensional plane laminar jet impinging normally onto a plate was done. A potential flow solution for an impinging liquid jet with uniform velocity profile was used to obtain information on the free stream velocity over the flat plate that serves as input for the boundary layer equations. A finite-difference method was used. A comparison of local Nusselt number distributions at various Reynolds numbers is shown in Fig. 2. The data taken from [18] corresponds to a non-dimensional nozzle height of 3.0. It was found that beyond that nozzle height there is no further change in the hydrodynamics and heat transfer. Such a critical nozzle height is also obtained in the present study and the results shown in Fig. 2 correspond to that. Note that the Prandtl number in the present study is 5.545 instead of 5 used in [18]. The Nusselt number has been adjusted by using a functional form of $Pr^{0.376}$. The results from Eq. (11) at the stagnation point are also included. As shown in the figure, the numerical results obtained in the present study are in close agreement with those in the literature.

In [19], an analysis was made of the fluid flow and heat transfer characteristics associated with the impingement of a slot jet with a non-uniform velocity profile. It was noted that uniform exit velocity profiles are encountered when the jet issues from a short nozzle with a high contraction ratio. On the other hand, if the fluid stream is delivered by a tube of sufficient length, the velocity profile at the exit cross-section corresponds to fully developed flow. Consideration was given to velocity profiles for a fully developed laminar flow. An approach similar to that employed in [18] for a uniform velocity profile was used. The velocity field within the impinging jet was solved within the framework of an inviscid flow model. Results from the inviscid solution were used as input for the analysis of the boundary layer heat transfer on the impingement surface. However, the task of finding the inviscid flow solution was more formidable as the flow is not a potential flow. Instead of using a parabolic profile for a fully developed flow, a sinusoidal profile is used in order to keep the vorticity equation linear. The study was specifically applied to the stagnation region. The results presented in Fig. 3 have been adjusted for the parabolic velocity profile and the Prandtl number dependence. See [19] for more detail. The results for uniform jet are also included for comparison. The stagnation heat transfer coefficients for the parabolic jet are found to be almost twice as large as those for the uniform jet. The numerical results obtained in the present study are in close agreement with those from [19].

The main body of results on oblique jets corresponds to a Reynolds number of 5000 and encompasses

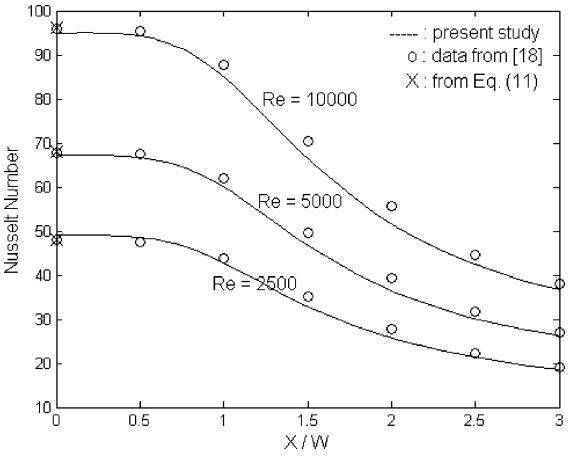

Fig. 2. Nusselt number comparison for a uniform jet at various Reynolds numbers.

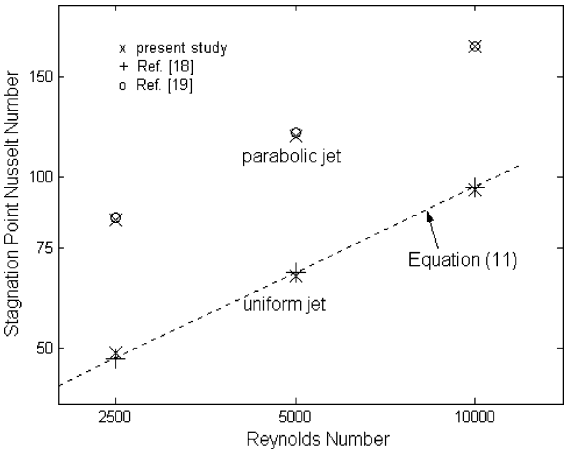

Fig. 3. Stagnation point Nusselt number comparison at various Reynolds numbers.

inclination angles of 90, 75, 60 and 45 deg. The influence of Reynolds number are explored by additional runs for $Re = 2500$ and 10,000. Uniform and parabolic jets are studied.

The free surface contours and the pressure distributions along the solid surface for various jet inclinations are shown in Fig. 4. As reported in the literature, the peak pressure location, which corresponds to the stagnation point, shifts upstream. The jet layer downstream thickens while the thickness of the layer upstream decreases as a result of reduced fluid flow caused by the jet inclination. Note that the shift in flow stagnation point and the downstream/upstream thickness ratio increase with the flow inclination.

A detailed flow field at the stagnation region of a 45-deg uniform jet, along with a dotted line corresponding to the pressure distribution at the wall, is shown in Fig. 5. It can be seen that the peak pressure location lies at the location of the stagnation point displayed by flow field. As mentioned previously, an analytical solution for the hydrodynamics of an oblique plane jet has been obtained in [6]. The predictions for the shift in P_{max} are plotted in Fig. 6 alongside the numerical results obtained in the present study. They appear to be in excellent agreement.

The local Nusselt number distributions along the solid surface are shown in Fig. 7. The corresponding isotherm distributions displaying the thermal boundary layers are given in Fig. 8. The peak Nusselt number increases and the distribution becomes increasingly asymmetric and shifting upstream as the inclination increases. This is in agreement with the results reported in [4] but is at variance with the results obtained for inclined air jets that show a decreasing trend in peak Nusselt number with inclination. The difference can be

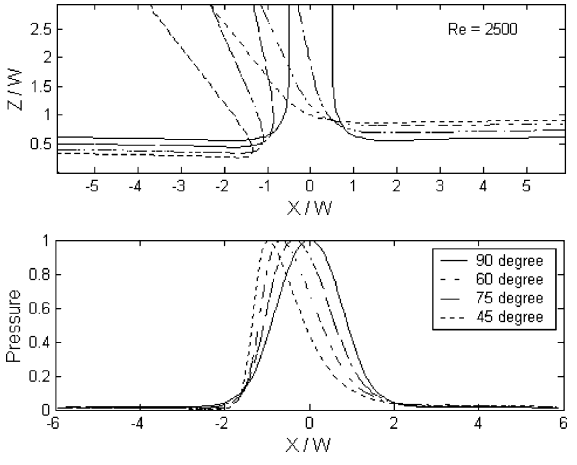

Fig. 4. Free surface and pressure profiles of a uniform jet at various jet inclinations.

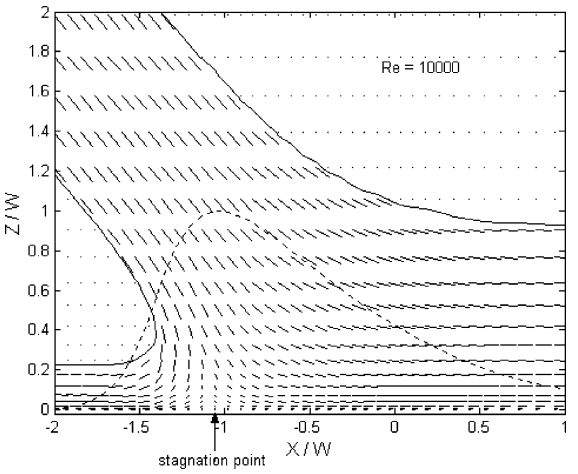

Fig. 5. Pressure distribution and flow field at the stagnation point region of a 45-deg uniform jet.

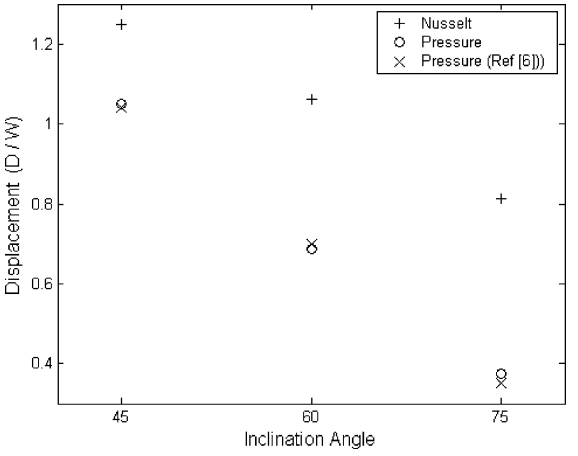

Fig. 6. Displacement of maximum Nusselt number and maximum pressure locations from the geometric center of impingement at various jet inclinations.

explained as a result of entrainment and jet spreading with submerged (air) jets. Entrainment has the effect of decreasing the average arrival velocity, and increasing the impingement area of the jet at the plate. The increased impingement area may account for the larger dimensionless shift in the point of maximum heat transfer for the submerged jets.

Furthermore, the heat transfer coefficient has been shown to be proportional to the spatial velocity gradient. An increase in jet inclination for a submerged jet will reduce the spatial velocity gradient near the point of maximum heat transfer as jet entrainment causes interaction between the jet flow and the plate on the upstream side, and increasing spread in the flow on the downstream side. The decrease in the velocity gradient

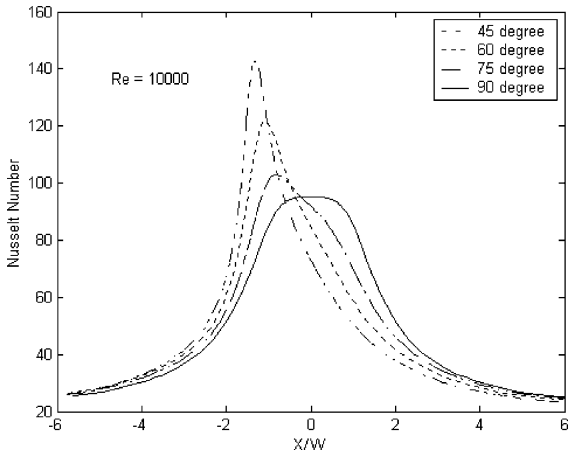

Fig. 7. Nusselt number distributions at various jet inclinations for a uniform jet.

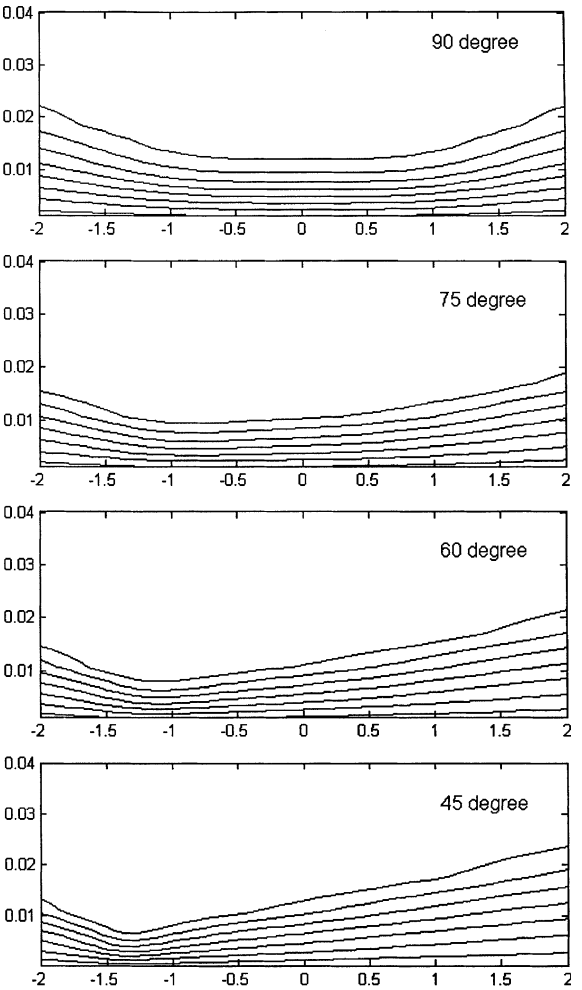

Fig. 8. Isotherm distributions at various inclinations of a uniform jet.

will lead to lower heat transfer previously observed for air jet [1–3].

As mentioned in [4], shear layer effects and entrainment are negligible for the free liquid jets. Increasing jet inclination results in an increasingly asymmetric flow pattern. This will lead to an increase in the spatial velocity gradient in the impingement region due to the required change in fluid flow direction of greater than 90 deg on the upstream side of the inclined jet. Hence, an increase in the Nusselt number is observed in contrast to the decrease found in submerged jets.

A flow field showing only the vertical velocity profiles at the stagnation region of a 45-deg uniform jet, along with a dotted line corresponding to the non-dimensionalized Nusselt number distribution at the wall, is shown in Fig. 9. Note that as the flow approaches the plate, the vertical velocity profile, which is uniform initially, tapers off at both ends as the jet spreads and develops a local peak upstream of the geometric center of the jet. A closer look at the figure reveals that the peak vertical velocity is located practically at the same position as that of the maximum Nusselt number. Note that, near the plate, as governed by the continuity equation, the vertical velocity component is proportional to the spatial velocity gradient. Therefore, the result shown in Fig. 9 is in agreement with the finding mentioned earlier that the heat transfer coefficient depends on the spatial velocity gradient.

The shift in Nu_{max} with inclination is plotted in Fig. 6 presented earlier. Note that the Nu_{max} location has a slightly larger shift than the stagnation point location. In [4], it was reported that, because of absence of entrainment, the magnitude of the shift was significantly less than that of the submerged jets for similar jet inclinations. The shift of maximum heat transfer location was

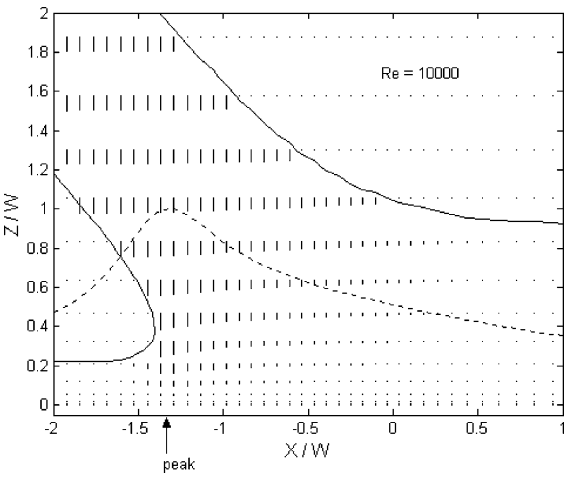

Fig. 9. Vertical velocity profiles at the maximum Nusselt number region of a 45-deg uniform jet.

only as large as the jet radius, which is much less than the numerical results obtained in the present study for the plane liquid jet. The difference is believed to be due to the geometry of the jet. The plane jet, being strictly two dimensional, is more confined compared to the circular jet, which is physically three dimensional. The flow will be forced upstream in a plane jet instead of sideway as in a circular jet case. Subsequently, a planar jet will have a larger shift than a circular jet. This can also explain the larger increase in maximum Nusselt number obtained for plane jets.

The effects of Reynolds number on the hydrodynamics and heat transfer of the oblique impingement have been examined. A sample plot showing the effect of Reynolds number is shown in Fig. 10. There is a slight increase in the shift in maximum Nusselt number location as the Reynolds number increases. As a whole, the Nusselt number is proportional to the square root of the Reynolds number. The three curves will collapse into one if the Nusselt numbers were normalized by the corresponding maximum Nusselt number. There is a slight increase in the shift of the stagnation point location as Reynolds number increases although the overall effect on the free surface contour and pressure distribution is minute.

So far, the results have all been on uniform jets. As previously mentioned, the heat transfer and the hydrodynamics of the impinging jet depend on the inlet velocity profile of the jet. A similar study has been performed for a parabolic jet. The results on the heat transfer are shown in Fig. 11. The most intriguing revelation is the initial decline and the subsequent rise in the maximum Nusselt number with the jet inclination. Obviously, the inlet velocity profile plays a key role in the flow and subsequently in the heat transfer.

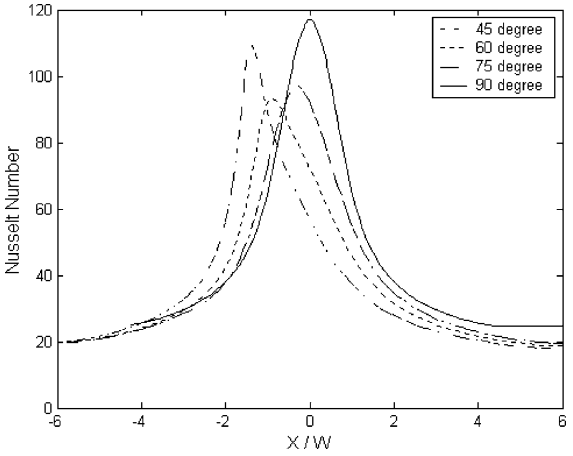

Fig. 11. Nusselt number distributions at various jet inclinations for a parabolic jet.

For the sake of comparison, Nusselt number distribution for both the uniform and the parabolic jet are put together in Fig. 12. It is understood that the inclination progresses as previously presented in Figs. 7 and 11 for the uniform and parabolic jet respectively. In the normal impingement case, as previously reported in Fig. 3, the Nusselt number is almost twice as large as that of a uniform jet. Also the flat zone at the stagnation point region for the uniform jet degenerates into a peak for the parabolic jet. At 75-deg inclination, besides a decline in the maximum Nusselt number for the parabolic jet, the shift for the maximum Nusselt number location is also less than that for the uniform jet. It should be noted that unlike the uniform jet case, the flow for the parabolic jet is more concentrated at the jet center. As the inclination begins, the peak spatial velocity gradient, which has a

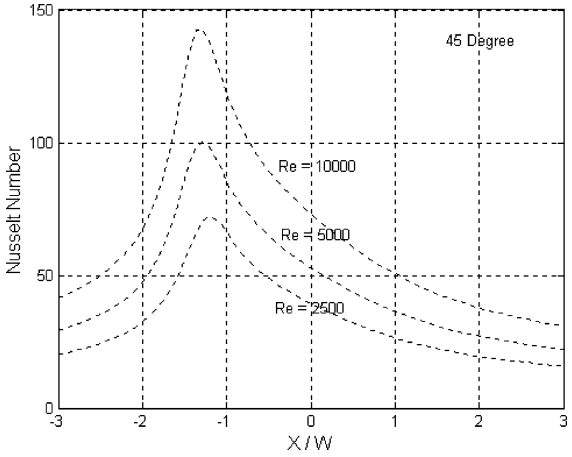

Fig. 10. Shift in maximum Nusselt number with Reynolds number of a uniform jet.

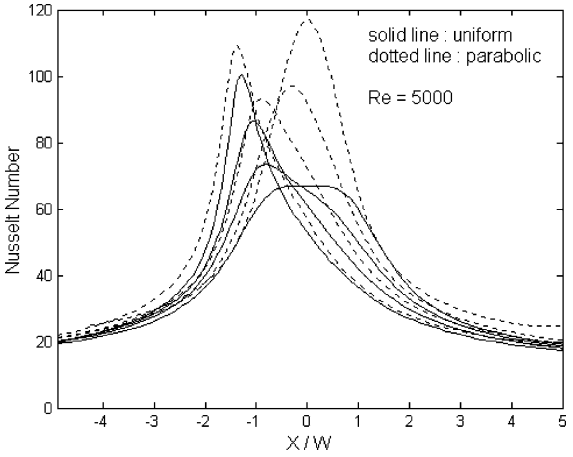

Fig. 12. Nusselt number comparisons between a uniform and a parabolic jet at various jet inclinations.

strong influence on the heat transfer, reduces in magnitude as it shifts upstream due to the uneven turning of the flow as it approaches the wall. In other words, the asymmetry of the oblique impingement, aided by the parabolic shape, eases the spatial velocity gradient and hence reduces the heat transfer. This trend continues and the influence propagates inward with declining magnitude as the inclination increases. Eventually, the trend will be reversed as more of the higher velocity fluid at the inner region is affected and required to turn. Note that the decline in maximum Nusselt number has reduced at 60 deg and the shift is closer to that of the uniform jet. At 45 deg, the maximum Nusselt number rises above that of 60 and 75 deg, although remains below that of the normal impingement (90 deg). In view of the numerical results obtained in the present study, the contradiction in findings previously mentioned between the two studies [4,5] might be a result of the jet inlet velocity profile.

4. Conclusions

A numerical study has been performed to examine the hydrodynamics and heat transfer mechanism of the impingement process of an oblique free liquid jet. Detailed flow fields as well as free surface contours and pressure distributions on the substrate have been obtained. Local Nusselt number distributions at the substrate have also been calculated. Uniform and parabolic jets have been considered. Both the maximum Nusselt number location and the maximum pressure location have been found to shift upstream from the geometrical impingement point of the jet, with the extent of the displacements increasing as the inclination increases. It has been found that the jet inlet velocity profile has a significant effect on the heat transfer. For uniform jets, the maximum Nusselt number increases as the inclination increases. For parabolic jets, the maximum Nusselt number initially declines and eventually rises as the jet inclination increases. The effects of Reynolds number on heat transfer of the oblique impingement have also been examined. As a whole, the Nusselt number is proportional to the square root of the Reynolds number. Results for normal impingement are also obtained and are in close agreement with experimental and analytical data obtained from the literature providing supports for the validity of the numerical study.

References

[1] E.M. Sparrow, B.J. Lovell, Heat transfer characteristics of an obliquely impinging circular jet, J. Heat Transfer 102 (1980) 202–209.

[2] R.J. Goldstein, M.E. Franchett, Heat transfer from a flat surface to an oblique impinging jet, J. Heat Transfer 110 (1988) 84–90.

[3] X. Yan, N. Saniei, Heat transfer from an obliquely impinging circular air jet to a flat plate, Int. J. Heat Fluid Flow 18 (1997) 591–599.

[4] J. Stevens, B.W. Webb, The effect of inclination on the local heat transfer under an axisymmetric, free liquid jet, Int. J. Heat Mass Transfer 34 (1991) 1227–1236.

[5] C.F. Ma, Q. Zheng, H. Sun, K. Wu, T. Gomi, B.W. Webb, Local characteristics of impingement heat transfer with oblique round free-surface jets of large Prandtl number liquid, Int. J. Heat Mass Transfer 40 (1997) 2249–2259.

[6] W. Schach, Umlenkung eines freien Flussigkeitsstrahles an einer ebenen Platte, Ing. Arch. 5 (1934) 245–265.

[7] B.R. Holt, A.Y. Tong, Numerical simulation of a liquid metal droplet impacting onto a rigid substrate, Fourth ASME/JSME Thermal Engineering Joint Conference, vol. 2, 1995, pp. 149–156.

[8] B.R. Holt, A.Y. Tong, The normal incidence impact and solidification phenomena of a liquid droplet onto a rigid substrate, Proceedings of the ASME Fluids Engineering Division, 1995 IMECE, FED-Vol. 234, 1995, pp. 215–224.

[9] A.Y. Tong, B.R. Holt, A numerical correlation for the solidification of liquid droplets impacting onto a substrate, Second International Symposium on Multiphase Flows and Heat Transfer on Materials Processing; 1996 IMECE, FED-Vol. 240, 1996, pp. 257–264.

[10] A.Y. Tong, B.R. Holt, Numerical study on the solidification of liquid metal droplets impacting onto a substrate, Numer. Heat Transfer, Part A 31 (1997) 797–817.

[11] A.Y. Tong, A numerical study on the collision behavior of droplets, Forum on Advances in Numerical Modeling of Free Surface and Interface Fluid Dynamics, FED-Vol. 238, Fluids Engineering Division Conference, vol. 3, 1996.

[12] M. Rudman, Volume-tracking methods for interfacial flow calculations, Int. J. Numer. Meth. Fluids 24 (1997) 671–691.

[13] D.S. Kershaw, The incomplete Cholesky-conjugate gradient method for the iterative solution of systems of linear equations, J. Comput. Phys. 26 (1978) 43–65.

[14] C.W. Hirt, B.D. Nichols, Volume of fluid (VOF) method for the dynamics of free boundaries, J. Comput. Phys. 39 (1981) 201–225.

[15] D.L. Youngs, Time-dependent multi-material flow with large fluid distortion, Numerical Methods for Fluid Dynamics, Academic, New York, 1982, pp. 273–285.

[16] J.U. Brackbill, D.B. Kothe, C. Zemach, A continuum method for modeling surface tension, J. Comput. Phys. 100 (1992) 335–354.

[17] B.W. Webb, C.F. Ma, Single-phase liquid jet impingement heat transfer, Adv. Heat Transfer 26 (1995) 105–217.

[18] H. Miyazaki, E. Silberman, Flow and heat transfer on a flat plate normal to a two-dimensional laminar jet issuing from a nozzle of finite height, Int. J. Heat Mass Transfer 15 (1972) 2097–2107.

[19] E.M. Sparrow, L. Lee, Analysis of flow field and impingement heat/mass transfer due to a nonuniform slot jet, J. Heat Transfer 97 (1975) 191–197.